RSC Advances

PAPER

View Article Online
View Journal | View Issue

Cite this: *RSC Adv.*, 2020, **10**, 5191

Regioselective convergent synthesis of 2-arylidene thiazolo[3,2-*a*]pyrimidines as potential anti-chikungunya agents†

Mohamed Fares, *[ab] Patrick M. McCosker, [ac] Muhammad A. Alsherbiny, [d] Anthony C. Willis, [e] Timothy Clark, [c] Johan Neyts, [f] Dirk Jochmans [f] and Paul A. Keller *[a]

Received 27th November 2019
Accepted 17th January 2020

DOI: 10.1039/d0ra00257g

rsc.li/rsc-advances

Convergent and convenient regioselective synthesis of novel thiazolo[2,3-*a*]pyrimidine derivatives was accomplished using the one-pot reaction of 6-ethylthiouracil, bromoacetic acid, anhydrous sodium acetate, acetic anhydride, acetic acid and suitable aldehyde. X-ray crystallographic study reveals the presence of the *Z* configuration of only one regioisomer confirmed by computational studies as being the most likely isomer present.

Arboviruses mainly use arthropod vectors for transmission between hosts and they are considered a growing global health threat.[1,2] This arises from the increasing number of travellers, from 450 million in 1990 to nearly 1.4 billion in 2018, and consequently travel-related diseases incidence has increased significantly.[3] Chikungunya virus (CHIKV) (*Alphavirus* genus, family Togaviridae) is one of the prevalent tropical alphaviruses that is transmitted by *Aedes* mosquitoes.[4,5] After an incubation period of 2–4 days, symptoms start with the onset of high fever and severe persistent joint pain that may last for weeks to years.[6,7] Other symptoms of chikungunya fever (CHIKF) include headache, vomiting, rash, myalgia (muscle pain), photophobia and maculopapular rash.[6,8] Unlike other arbovirus infections, around 15% of the patients may encounter "silent infections".[6]

A variety of strategies have been applied to develop anti-CHIKV treatments, including vaccines, and for small molecule inhibitors, random screening, computer aided drug design, ligand-based drug design, high throughput screening and genome-wide loss of function screen.[9–17] Non-steroidal anti-inflammatory drugs (NSAID) have been used to alleviate the symptoms of the CHIKF because of the lack of effective prevention or curing of the viral infection.[18] However, so far there is no vaccine or approved medication to prevent or treat CHIKV infection.

The recent advances and growing knowledge about the arboviruses expand our understanding of the CHIKV life cycle, pathogenesis and infection.[1–6] Intensive research in the past 10 years has led to the identification of new chemical scaffolds that might be potential anti-CHIKV agents. Rhodanine **I** is a thiazolidin-4-one derivative, presenting a scaffold that exhibited broad antiviral activity against HCV, HIV-1 and Chikungunya (Fig. 1).[19] A series of rhodanine derivatives was tested for their anti-CHIKV activity by a cytopathic effect (CPE) reduction assay (Fig. 1). The 2-methyl analogue **II** emerged as the best compound and displayed excellent activity with submicromolar

[a]*School of Chemistry & Molecular Bioscience, Molecular Horizons, University of Wollongong, Illawarra Health & Medical Research Institute, Wollongong, NSW 2522, Australia. E-mail: Ph.fares@yahoo.com; keller@uow.edu.au*

[b]*School of Chemistry, The University of Sydney, NSW 2006, Australia*

[c]*Department of Chemistry and Pharmacy, Computer-Chemistry-Center (CCC), Friedrich-Alexander-Universität Erlangen-Nürnberg (FAU), Nägelbachstrasse 25, 91052 Erlangen, Germany*

[d]*NICM Health Research Institute, Western Sydney University, Westmead, NSW 2145, Australia*

[e]*Research School of Chemistry, The Australian National University, Canberra, ACT 2601, Australia*

[f]*KU Leuven (University of Leuven), Department of Microbiology and Immunology, Rega Institute for Medical Research, Laboratory of Virology and Chemotherapy, B-3000, Leuven, Belgium*

† Electronic supplementary information (ESI) available. CCDC 1968317. For ESI and crystallographic data in CIF or other electronic format see DOI: 10.1039/d0ra00257g

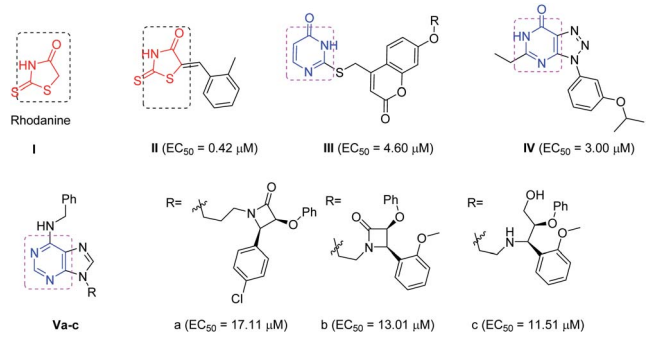

Fig. 1 Examples of heterocyclic classes showing anti-CHIKV activity, including thiazolidin-4-one **I** and **II**, pyrimidine **III** and pyrimidine fused rings **IV** and **IVa–c**.

EC_{50} (EC_{50} = 0.42 μM) against CHIKV. A docking study also showed good interaction between the ligand and CHIKV nsp2 protease.[19]

Among the main heterocycles that form the basis of small molecule inhibitors of CHIKV are the pyrimidine and fused pyrimidine rings, *e.g.* **III**, **IV** and **Va–c** (Fig. 1).[15,20,21] Recent reports indicated that hybridization between uracil–coumarin–arenes **III** resulted in the discovery of a novel anti-CHIKV scaffold that was found to impede CHIKV replication.[20] In an effort to find new leads as CHIKV inhibitors, a random screening identified the [1,2,3]triazolo[4,5-*d*]pyrimidin-7(6*H*)ones as potential candidates.[21] Iterative optimization cycles led to the most potent compound **IV** with EC_{50} = 3 μM and a selectivity index greater than 600 (Fig. 1).[21] In 2012, purine-β-lactams **Va** and **Vb** and purine-amino propanol **Vc** (Fig. 1) conjugates were screened against nine different viruses including CHIKV. The amino propanol derivative **Vc** (EC_{50} = 11.51–17.11 μM) showed relatively higher activity other than the purine-β-lactam hybrids. Therefore, the β-lactam was not essential for activity.[15]

Recently, hybridization of two or more bioactive fragments has emerged as a concept for the exploration of novel multi-target acting inhibitors as well as novel anti CHIKV agents (Fig. 2).[15,20,22,23] Therefore, in our ongoing efforts to discover new scaffolds for CHIKV infection, we investigated a molecular hybridization approach with the fusion of the uracil and the rhodanine pharmacophoric moieties (Fig. 2).[22]

The synthetic strategy started with the condensation of ethyl propionylacetate **1** and thiourea **2** to afford the known 6-ethyl thiouracil **3** with 69% yield.[24,25] Although the synthesis of the thiazolopyrimidine derivatives from the 6-ethylthiouracil substrate has not previously been reported, this multicomponent reaction (MCR) was achieved using an analogous procedure[26–29] by reacting **3** with the aldehyde, chloroacetic acid, sodium acetate anhydrous, acetic anhydride and acetic acid in one pot and at reflux for 4 h (Scheme 1).

These conditions consistently gave low yields and two regioisomers (*e.g.* chlorobenzaldehyde **8** A : B 16% : 84%), the latter determined by analysis of the ^{1}H NMR spectrum (Fig. 3) – attempts to separate the isomers by column chromatography failed.

Optimization of the reaction involved varying the mode of addition, replacement of the chloroacetic acid with bromoacetic

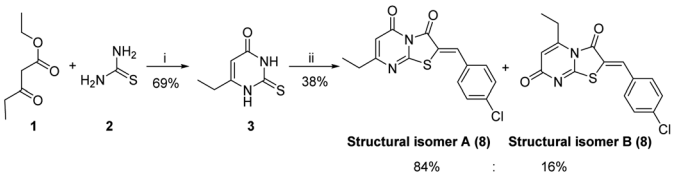

Scheme 1 Reagents and conditions: (i) NaOEt, C_2H_5OH, 6 h, reflux; (ii) $ClCH_2COOH$, anhydrous CH_3COONa, $(CH_3CO)_2$, CH_3COOH, 4-chlorobenzaldehyde, reflux, 4 h.

acid, and lowering the reaction temperature. This aimed to favour the formation of the kinetic regioisomer (*Z*)-A, assumed to be the desired product, over the thermodynamic regioisomer (*Z*)-B (Scheme 2), and resulted in the crystallization of only one regioisomer from the reaction mix (acetic acid) in each case. This may be due to the low reactivity and the less regioselectivity of the chloroacetic acid compared to bromoacetic acid.

From the convergent reaction conditions, four possible isomers can be formed: the *Z* or *E* configurations of structural isomers A or B – (*Z*)-A, (*E*)-A, (*Z*)-B and (*E*)-B (Fig. 4). Analysis of the ^{1}H NMR spectra showed a quartet at 2.48–2.57 ppm assigned to methylene hydrogens of the ethyl substituent – these were assigned to structural isomer A as the corresponding resonances of isomer B are expected to resonate more downfield (~3 ppm) as a result of a deshielding anisotropic effect of the adjacent carbonyl group of the thiazole ring.

The *Z* absolute configuration of this class of molecules was confirmed by X-ray crystallographic analysis of derivative **12** (Fig. 5). This illustrated the planarity of the thiazolopyrimidine rings with the aryl group, which may be attributed to two intramolecular hydrogen bonds. The *Z*-configuration is presumably stabilized by the two intramolecular hydrogen bonds between the arylidene H and the oxygen atom of the thiazole carbonyl group (HB1) and between the sulfur atom and the aryl hydrogen (HB2). The distance of both hydrogen bonds is 2.49 and 2.50 Å, for HB1 and HB2, respectively, and the angles are 102.81° and 132.94° for HB1 and HB2 respectively.

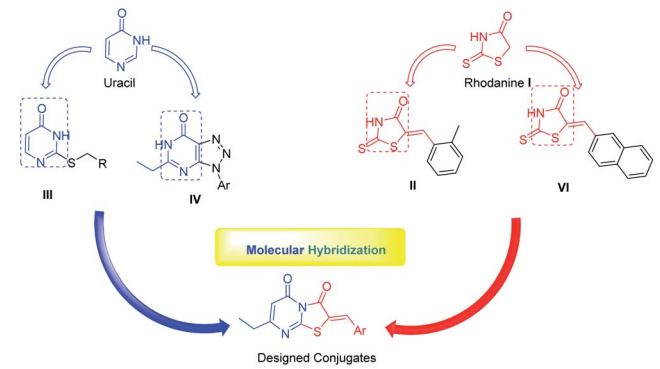

Fig. 2 Design of the targeted uracil–rhodanine conjugates.

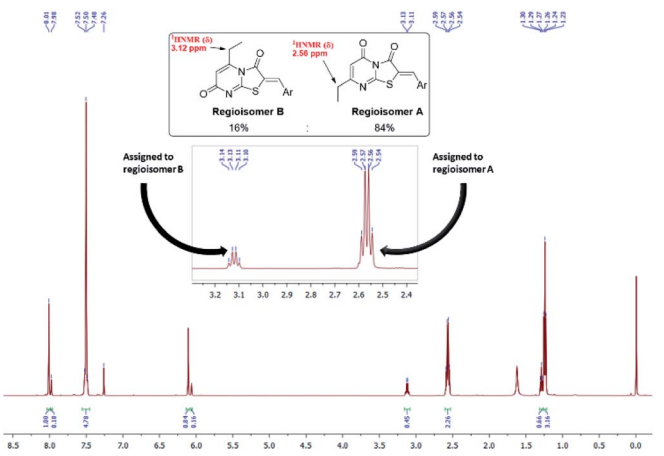

Fig. 3 ^{1}H NMR spectrum of the MCR product of the two regioisomers of **8** in a ratio of 1 : 5.

#	Ar	yield (%)
6	$-C_6H_5$	39
7	$4\text{-}FC_6H_4$	40
8	$4\text{-}ClC_6H_4$	48
9	$4\text{-}CH_3C_6H_4$	37
10	$4\text{-}OCH_3C_6H_4$	44
11	1-naphthyl	70
12	$4\text{-}OAc\text{-}3\text{-}OCH_3\ C_6H_3$	59
13	$3,4\text{-}(CH_2O_2)C_6H_3$	67
14	$4\text{-}C_6H_5\text{-}C_6H_4$	77
15	$4\text{-}(4\text{-}CH_3C_6H_4)C_6H_4$	69
16	2-pyrrolo	27
17	2-thieno	43
18	5-nitro-2-furo	46
19	2-pyridyl	22
20	7-indolyl	37

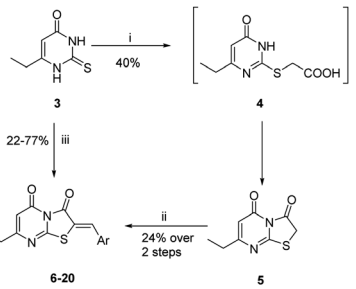

Scheme 2 Reactions and conditions: (i) $BrCH_2COOH$, anhydrous CH_3COONa, $(CH_3CO)_2$, CH_3COOH, 60 °C, 3 h; (ii) benzaldehyde, anhydrous CH_3COONa, CH_3COOH, 60 °C, 2 h. (iii) $BrCH_2COOH$, anhydrous CH_3COONa, $(CH_3CO)_2$, CH_3COOH, aldehyde, 60 °C, 4 h.

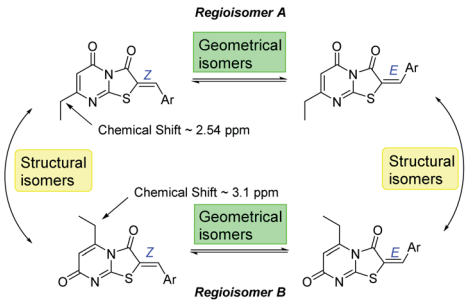

Fig. 4 The four possible isomers that can be produced from the MCR reaction.

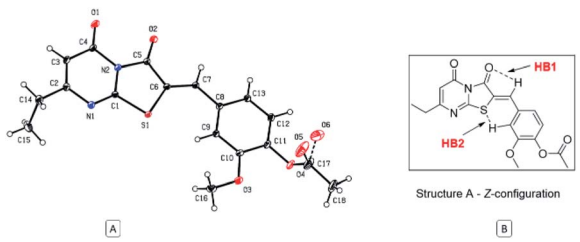

Fig. 5 (A) ORTEP diagram of compound **12**, (B) representation of stabilizing hydrogen bonds of the regioisomer (*Z*)-A.

To investigate the observed preference for the *Z* isomer, density functional theory (DFT) calculations were performed using the widely applied M06-2X functional with a Dunnings aug-cc-pVDZ basis set. Compound **6** (Ar = C_6H_6) was selected for the theoretical study and all structures were optimised with modelled acetic acid solvation (SMD). Analysis of the proposed mechanism indicated a possible alcohol intermediate and dehydration step preceded the final *Z*/*E* isomer formation, and to keep the model simple, the calculations have focussed on these molecules only, maintaining chirality where applicable (Fig. S1†). Conformer analysis of the alcohol intermediate indicated a Gibbs free energy of reaction ($\Delta_r G^0${298 K}) range of +0.35 to −2.30 kcal mol^{-1} with the *Z* arranged **C1** being the lowest and the *E* arranged **C2** the highest energy conformers respectively (Fig. S2†). Analysis of the optimised geometries gave no indication of hydrogen bond stabilisation for the alcohol, despite attempts at manually inputting the conformation. This indicated steric and geometric arrangement of the alcohol intermediate is more significant for the energy term.

A stacked ring conformer (**C3**) was also observed with a favourable $\Delta_r G^0${298 K} of −1.30 kcal mol^{-1}. To better account for this interaction, Grimme's dispersion (D3) and geometric counterpoise (gCP) corrections[30] were applied to the energy term, and the stacked **C3** was observed to increase by +1.29 kcal mol^{-1}, whereas **C1**/**C2** increased by +0.87 and +0.85 kcal mol^{-1} respectively. The similar increase to the energy term for **C1**/**C2** suggested there are no differences in dispersion effects to account for in these conformers. However, the greater energy change observed with **C3** was indicative the ring stacking is not a favourable intramolecular force. Based on the subtle differences in energies of the conformers, **C1** is the apparent favoured alcohol intermediate conformer, which is arranged to dehydrate to the *Z* isomer.

The transition states of the proposed dehydration reactions were calculated and the saddle point $\Delta_r G^0${298 K} were found to be +32.58 and +30.05 kcal mol^{-1} for the *E* **T1** and *Z* **T2** arranged transition states respectively (Fig. S3a†). With the D3-gCP corrections $\Delta_r G^0${298 K} were +33.51 and +30.90 kcal mol^{-1} for **T1** and **T2** respectively. The similar increases in energy (+0.93 and +0.85 kcal mol^{-1}) indicated negligible differences in dispersion force correction required when comparing **T1** and **T2**. What was particularly interesting to note, in contrast to the alcohol intermediate, is the preference of the water leaving hydrogen bound to the carbonyl. Despite attempts in manually positioning the water to leave adjacent to the sulfur, and in turn have H–S interaction, the transition state only converged to allow hydrogen bonding of the water with the thiazole carbonyl. Subsequently, it was proposed the principal factor dictating the favoured transition state is the arrangement of the aryl group, as the water has apparent preference for leaving *trans* to the sulfur, in favour of *Z* isomer formation.

Subsequent calculation of the product (*E*)-**6** and (*Z*)-**6** isomers indicated $\Delta_r H^0${298 K} of −2.40 and −6.78 kcal mol^{-1} respectively, which indicts the *Z* isomer to be thermodynamically favoured, and D3-gCP corrections were in good agreement (Fig. 6 and S3b†). Comparison of the calculated (*Z*)-**6** structure with the X-ray crystal structure of compound **12** indicated similar bond distances of HB1 = 2.43 Å and HB2 = 2.50 Å for the proposed intramolecular hydrogen bonds (Fig. 5).

Likewise, the bond angles were in good agreement for HB1 and HB2 calculated at 101.34° and 127.70°, compared with 102.81° and 132.94° from the crystal structure, respectively. In conclusion, although the energy differences are small between the investigated reaction pathways, there is a consistent preference for the *Z* forming pathway at each step investigated and this result was reciprocated by D3-gCP energy corrections (Fig. 6).

The compounds were screened for their antiviral activities in a viral-cell based assay against Chikungunya virus (Indian Ocean strain 899) (Table S1†).

Based on the biological results, compounds **6–20** showed different percentages of viral replication inhibition at

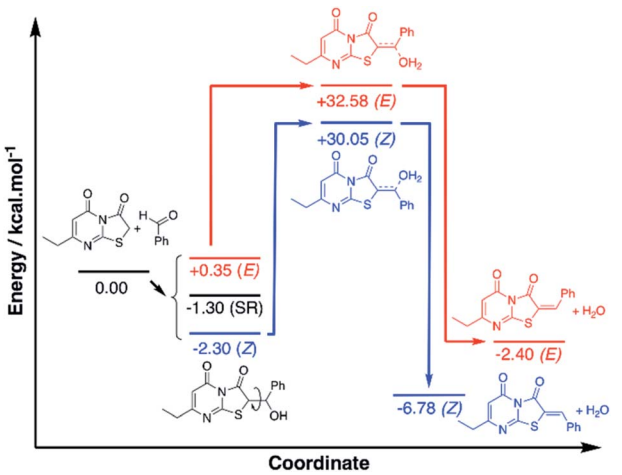

Fig. 6 Energy profile for the formation of compound **6**(*Z*) and **6**(*E*), calculated with DFT M06-2X/aug-cc-pVDZ. Divergent reaction pathways are color coded red for *E* formation and blue for *Z* formation. SR = stacked rings conformer.

20 μg mL^{-1} with (*Z*)-7-ethyl-2-((4′-methyl-[1,1′-biphenyl]-4-yl) methylene)-5*H*-thiazolo[3,2-*a*]pyrimidine-3,5(2*H*)-dione showing the best activity with 58% inhibition of CHIKV replication. Derivatives **6**, **11** and **20** showed 19, 28 and 34% inhibition of viral replication, while rest of the compounds showed fair or no activity. However, thiazolodione **15** can be considered as a potential lead compound in our future iterative cycles of optimization. The compound emerged as the most promising antiviral among the tested series with $EC_{50} = 42$ μM, with $IC_{50} >$ 250 μM against the breast cancer cell line MCF-7 and the endothelial human sapiens cell line EA.hy926. Compound **15** is endowed with *p*-methylbiphenyl tail functionality which might interact favourably with the target. Our outlook will include optimization of compound **15** with the prime aim to find safe and effective anti-CHIKV agents.

In this paper, we shed the light to the convergent synthesis of a new series of 2-arylidene thiazolo[3,2-*a*]pyrimidines. Using simple synthons, namely 6-ethylthiouracil, bromoacetic acid and different aldehydes in a mixture of acetic acid/acetic anhydride and catalytic amount of anhydrous sodium acetate, a novel series of (*Z*)-7-ethyl-2-arylidine-5*H*-thiazolo[3,2-*a*]pyrimidine-3,5(2*H*)-diones was achieved. Optimization of the multi component reaction conditions by replacing chloroacetic acid with the more regioselective bromoacetic acid, lowering reaction temperature and changing the mode of addition and we were able to prepare one isomer at each case. X-ray crystal structure of compound **12** shows that only one regioselective isomer formed with the *Z* configuration that is potentially stabilized by two intramolecular hydrogen bonds. Antiviral activity evaluation demonstrated the tailed thiazolopyrimidine **15** as a candidate for future development.

Conflicts of interest

There are no conflicts to declare.

Acknowledgements

MF thanks UOW for the University Postgraduate Award and International Postgraduate Tuition Award scholarships.

References

1 A. Cifuentes Kottkamp, E. De Jesus, R. Grande, J. A. Brown, A. R. Jacobs, J. K. Lim and K. A. Stapleford, *J. Virol.*, 2019, **93**, e00389-19.
2 Y. S. Huang, S. Higgs and D. L. Vanlandingham, *Front. Microbiol.*, 2019, **10**, 22.
3 C. B. F. Vogels, C. Ruckert, S. M. Cavany, T. A. Perkins, G. D. Ebel and N. D. Grubaugh, *PLoS Biol.*, 2019, **17**, e3000130.
4 A. A. Rashad, S. Mahalingam and P. A. Keller, *J. Med. Chem.*, 2014, **57**, 1147–1166.
5 B. J. Matthews, O. Dudchenko, S. B. Kingan, S. Koren, I. Antoshechkin, J. E. Crawford, W. J. Glassford, M. Herre, S. N. Redmond, N. H. Rose, G. D. Weedall, Y. Wu, S. S. Batra, C. A. Brito-Sierra, S. D. Buckingham, C. L. Campbell, S. Chan, E. Cox, B. R. Evans, T. Fansiri, I. Filipovic, A. Fontaine, A. Gloria-Soria, R. Hall, V. S. Joardar, A. K. Jones, R. G. G. Kay, V. K. Kodali, J. Lee, G. J. Lycett, S. N. Mitchell, J. Muehling, M. R. Murphy, A. D. Omer, F. A. Partridge, P. Peluso, A. P. Aiden, V. Ramasamy, G. Rasic, S. Roy, K. Saavedra-Rodriguez, S. Sharan, A. Sharma, M. L. Smith, J. Turner, A. M. Weakley, Z. Zhao, O. S. Akbari, W. C. t. Black, H. Cao, A. C. Darby, C. A. Hill, J. S. Johnston, T. D. Murphy, A. S. Raikhel, D. B. Sattelle, I. V. Sharakhov, B. J. White, L. Zhao, E. L. Aiden, R. S. Mann, L. Lambrechts, J. R. Powell, M. V. Sharakhova, Z. Tu, H. M. Robertson, C. S. McBride, A. R. Hastie, J. Korlach, D. E. Neafsey, A. M. Phillippy and L. B. Vosshall, *Nature*, 2018, **563**, 501–507.
6 O. Schwartz and M. L. Albert, *Nat. Rev. Microbiol.*, 2010, **8**, 491–500.
7 Y. Villero-Wolf, S. Mattar, A. Puerta-Gonzalez, G. Arrieta, C. Muskus, R. Hoyos, H. Pinzon and D. Pelaez-Carvajal, *Sci. Rep.*, 2019, **9**, 9970.
8 P. Mahendradas, K. Avadhani and R. Shetty, *J. Ophthalmic Inflammation Infect.*, 2013, **3**, 35.
9 L. J. Chang, K. A. Dowd, F. H. Mendoza, J. G. Saunders, S. Sitar, S. H. Plummer, G. Yamshchikov, U. N. Sarwar, Z. Hu, M. E. Enama, R. T. Bailer, R. A. Koup, R. M. Schwartz, W. Akahata, G. J. Nabel, J. R. Mascola, T. C. Pierson, B. S. Graham, J. E. Ledgerwood and V. R. C. S. Team, *Lancet*, 2014, **384**, 2046–2052.
10 T. Agarwal, S. Asthana and A. Bissoyi, *Indian J. Pharm. Sci.*, 2015, **77**, 453–460.
11 P. T. Nguyen, H. Yu and P. A. Keller, *J. Mol. Model.*, 2014, **20**, 2216.
12 R. K. Maheshwari, V. Srikantan and D. Bhartiya, *J. Virol.*, 1991, **65**, 992–995.
13 P. T. Nguyen, H. Yu and P. A. Keller, *J. Mol. Graphics Modell.*, 2015, **57**, 1–8.

14 A. Karlas, S. Berre, T. Couderc, M. Varjak, P. Braun, M. Meyer, N. Gangneux, L. Karo-Astover, F. Weege, M. Raftery, G. Schonrich, U. Klemm, A. Wurzlbauer, F. Bracher, A. Merits, T. F. Meyer and M. Lecuit, *Nat. Commun.*, 2016, **7**, 11320.

15 M. D'Hooghe, K. Mollet, R. De Vreese, T. H. Jonckers, G. Dams and N. De Kimpe, *J. Med. Chem.*, 2012, **55**, 5637–5641.

16 K. M. Feibelman, B. P. Fuller, L. Li, D. V. LaBarbera and B. J. Geiss, *Antiviral Res.*, 2018, **154**, 124–131.

17 A. Gomez-SanJuan, A. M. Gamo, L. Delang, A. Perez-Sanchez, S. N. Amrun, R. Abdelnabi, S. Jacobs, E. M. Priego, M. J. Camarasa, D. Jochmans, P. Leyssen, L. F. P. Ng, G. Querat, J. Neyts and M. J. Perez-Perez, *ACS Infect. Dis.*, 2018, **4**, 605–619.

18 H. A. Rothan, H. Bahrani, A. Y. Abdulrahman, Z. Mohamed, T. C. Teoh, S. Othman, N. N. Rashid, N. A. Rahman and R. Yusof, *Antiviral Res.*, 2016, **127**, 50–56.

19 S. S. Jadav, B. N. Sinha, R. Hilgenfeld, B. Pastorino, X. de Lamballerie and V. Jayaprakash, *Eur. J. Med. Chem.*, 2015, **89**, 172–178.

20 J. R. Hwu, M. Kapoor, S. C. Tsay, C. C. Lin, K. C. Hwang, J. C. Horng, I. C. Chen, F. K. Shieh, P. Leyssen and J. Neyts, *Antiviral Res.*, 2015, **118**, 103–109.

21 A. Gigante, M. D. Canela, L. Delang, E. M. Priego, M. J. Camarasa, G. Querat, J. Neyts, P. Leyssen and M. J. Perez-Perez, *J. Med. Chem.*, 2014, **57**, 4000–4008.

22 M. Fares, W. M. Eldehna, S. M. Abou-Seri, H. A. Abdel-Aziz, M. H. Aly and M. F. Tolba, *Arch. Pharm.*, 2015, **348**, 144–154.

23 J. R. Hwu, W. C. Huang, S. Y. Lin, K. T. Tan, Y. C. Hu, F. K. Shieh, S. O. Bachurin, A. Ustyugov and S. C. Tsay, *Eur. J. Med. Chem.*, 2019, **166**, 136–143.

24 J. P. Spengler and W. Schunack, *Arch. Pharm.*, 1984, **317**, 425–430.

25 M. Fares, S. M. Abou-Seri, H. A. Abdel-Aziz, S. E. Abbas, M. M. Youssef and R. A. Eladwy, *Eur. J. Med. Chem.*, 2014, **83**, 155–166.

26 M. M. Mohamed, A. K. Khalil, E. M. Abbass and A. M. El-Naggar, *Synth. Commun.*, 2017, **47**, 1441–1457.

27 A.-S. M. Abdel-fattah, A. M. Negm and A. E. Mustafa Gaafar, *Phosphorus, Sulfur, and Silicon and the Related Elements*, 1992, **72**, 145–156.

28 A. Hamouda, *Der Pharma Chem.*, 2014, **6**, 346–357.

29 E. Abdelghani, S. A. Said, M. Assy and A. M. A. Hamid, *J. Iran. Chem. Soc.*, 2015, **12**, 1809–1817.

30 H. Kruse and S. Grimme, *J. Chem. Phys.*, 2012, **136**, 154101.